Proc. Annual Meeting of the Austrian Society for Biomedical Engineering 2021
DOI: 10.3217/978-3-85125-826-4-20

DIRECTED CONNECTIVITY ANALYSIS IN PEOPLE WITH SPINAL CORD INJURY DURING ATTEMPTED ARM AND HAND MOVEMENTS

Kyriaki Kostoglou[1], Gernot Müller-Putz[1]

[1]Institute of Neural Engineering, Graz University of Technology, Austria

kkostoglou@tugraz.at

Abstract— *We investigated the cortical connectivity patterns that arise in subjects with spinal cord injury (SCI) during attempted hand and arm movements using multivariate autoregressive (MVAR) models and electroencephalographic (EEG) signals. The MVAR models were fitted using multiple trials from multiple subjects in order to capture general connectivity characteristics during different type of attempted movements. Based on the results we detected two main sources of information: the somatosensory and the primary motor area. Changes in directional connectivity between different regions before and after cue onset were found to be informative in terms of the type of movement attempted by the SCI participants.*

Keywords— *multivariate autoregressive model, directed coherence, EEG, spinal cord injury, attempted movement*

Introduction

Multivariate autoregressive (MVAR) models have been extensively used to capture couplings between different time-series [1]–[3]. They provide measures of interdependency but also causality in the frequency domain, which is an important aspect when investigating directional connectivity in the brain (i.e., how brain regions send and receive information).

Herein, we applied MVAR analysis in electroencephalographic (EEG) signals projected, however, on the source space for improved localization of brain sources. The EEG signals were acquired from spinal cord injury (SCI) subjects during attempted arm and hand movements. It has been previously suggested that motor cortex areas in SCI subjects can be activated during motor attempts of the paralyzed limbs [4]. This has enabled the use of EEG-based brain-computer interfaces (BCI) to enhance restoration of movements lost after SCI [5], [6]. Our analysis was mainly exploratory, and our main goal was to capture general oscillatory interactions between different cortex regions before and after cue onset. To our knowledge, there has been only one study by Astolfi et al. [7] that has investigated SCI connectivity during attempted foot movements using MVAR models. Herein, we focused on detecting possible connectivity patterns that can be linked to the different type of attempted hand/arm movements. This information is important in order to establish MVAR-based measures as possible features for BCI applications.

Methods

Data Acquisition

61-channel EEG signals were obtained from 10, originally right-handed, SCI participants (median age of 54±18.5) as described in [5] (available at https://doi.org/10.1038/s41598-019-43594-9). The neurological level of injury ranged from C1-C7. At the beginning of each trial, a fixation cross was initially presented on a black screen, along with a beep sound. The class cue was displayed 2s after the trial initialization. The participants were asked to attempt unilaterally one of the following arm/hand movements: pronation, supination, palmar grasp, lateral grasp or hand open. Each trial lasted for 5s.

Data Preprocessing

The recorded EEG signals were pre-processed using EEGLAB and Matlab. First, we bandpass-filtered the signals between 0.3 and 70 Hz using a 4th order, zero-phase, Butterworth filter. Trials with dominant impulsive noise characteristics were rejected using thresholding, as well as techniques based on abnormal joint probabilities and kurtosis [5]. Next, we performed independent component analysis (ICA) to remove stationary artefactual components such as blinks, saccades, and muscle movements. Source localization was carried out in Brainstorm [8] using minimum norm imaging and sLoreta. To examine connectivity related to motor function, we extracted 26 spatially segregated signals (13 for the left hemisphere and 13 for the right hemisphere) from anatomical regions defined by the Brodmann atlas (Fig. 1). These 26 anatomical regions correspond to the somatosensory area, the primary motor area, the pre-motor area, the Broca's area, the visual area and the perirhinal area (Fig.1). The extracted signals were then used to fit MVAR models using multiple trials from all participants for different attempted movements.

MVAR

In an MVAR model, each variable is predicted by the linear combination of its past values, as well as the history of all other variables. An M-dimensional MVAR of order p can be expressed as [9],

$$\boldsymbol{y}(n) = \sum_{k=1}^{p} \boldsymbol{A}_k \boldsymbol{y}(n-k) + \boldsymbol{\varepsilon}(n) \qquad [1]$$

Published by Verlag der TU Graz
Graz University of Technology

DOI: 10.3217/978-3-85125-826-4-20

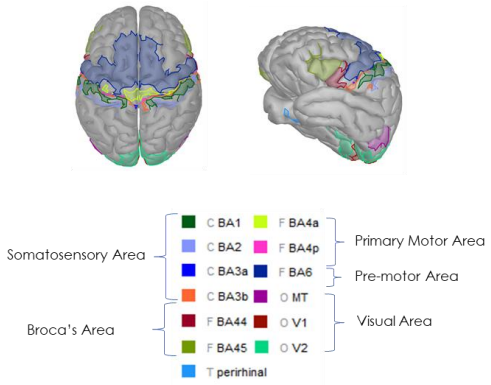

Somatosensory Area	BA1
	BA2
	BA3a
	BA3b
Primary Motor Area	BA4a (anterior)
	BA4p (posterior)
Pre-motor Area	BA6
Broca's Area	BA44 (pars opercularis)
	BA45 (pars triangularis)
Visual Area	MT (middle temporal)
	V1 (primary)
	V2 (secondary)
Perirhinal Area	BA35-BA36

Figure 1: Regions of Brodmann atlas

where $\boldsymbol{y}(n) = [y_1(n) \quad \dots \quad y_M(n)]^{\boldsymbol{T}} \in \boldsymbol{R}^{M\times 1}$ is a vector containing the values of M time-series at time n (i.e., the 26 source signals in our case). $\boldsymbol{A}_k$ is the so-called autoregressive matrix for $k = 1,..,p$ and $\boldsymbol{\varepsilon}(n)$ is the MVAR driving process noise which is assumed to be zero-mean and white. Equation 1 can be reformulated as,

$$\boldsymbol{y}(n) = \boldsymbol{A}\boldsymbol{\varphi}(n) + \boldsymbol{\varepsilon}(n) \qquad [2]$$

where $\boldsymbol{A} = [\boldsymbol{A}_1 \quad \dots \quad \boldsymbol{A}_p] \in \boldsymbol{R}^{M\times Mp}$ and $\boldsymbol{\varphi}(n) = [\boldsymbol{y}(n)^{\boldsymbol{T}} \quad \dots \quad \boldsymbol{y}(n-p)^{\boldsymbol{T}}]^{\boldsymbol{T}} \in \boldsymbol{R}^{Mp\times 1}$.
In this work, we used multiple trials from all participants to fit MVAR models that describe different type of attempted movements. Therefore, we expressed $\boldsymbol{y}(n)$ and $\boldsymbol{\varphi}(n)$ as,

$$\boldsymbol{y}(n) = [\boldsymbol{y}^1(n) \quad \dots \quad \boldsymbol{y}^K(n)]^{\boldsymbol{T}} \in \boldsymbol{R}^{M\times K} \qquad [3]$$

$$\boldsymbol{\varphi}(n) = \left[\boldsymbol{y}(n)^{\boldsymbol{T}} \quad \dots \quad \boldsymbol{y}(n-p)^{\boldsymbol{T}}\right] \in \boldsymbol{R}^{Mp\times K} \qquad [4]$$

where $\boldsymbol{y}(n)$ represents the M source signals concatenated from all K trials at time point n. The trial-based MVAR coefficients were computed using ordinary least-squares estimation.

MVAR model order selection

One important step in MVAR estimation is the selection of the model order p. Herein, we used the multivariate Akaike Information Criterion (AIC) defined as [10],

$$AIC(p) = N \cdot log\left(\left|\widehat{\boldsymbol{\Sigma}}\right|\right) + 2 \cdot d \qquad [5]$$

where N is the total number of samples, $\left|\widehat{\boldsymbol{\Sigma}}\right|$ is the determinant of the covariance of the residuals and $d = M^2p$ the total number of MVAR coefficients. The optimal p was selected by minimizing the AIC score described in Eq.(5).

MVAR coupling measures

To extract measures of coupling and directionality in the frequency domain, we applied the Fourier transform on Eq.2,

$$\boldsymbol{Y}(f) = \boldsymbol{H}(f)\boldsymbol{E}(f) = [\boldsymbol{I} - \boldsymbol{A}(f)]^{-1}\boldsymbol{E}(f) \qquad [6]$$

where $\boldsymbol{A}(f) = \sum_{k=1}^{p} \boldsymbol{A}_k\, e^{-i2\pi fkT}$ is the coefficient matrix and $\boldsymbol{H}(f) = [\boldsymbol{I} - \boldsymbol{A}(f)]^{-1} = \overline{\boldsymbol{A}}(f)^{-1}$ is the transfer matrix in the frequency domain. The relationship between $\boldsymbol{H}(f)$ and $\boldsymbol{A}(f)$ allows frequency domain measures of coupling to be derived easily using solely the coefficients of the MVAR model. The power spectral density matrix of the MVAR process can be written as,

$$\boldsymbol{S}(f) = \boldsymbol{H}(f)\boldsymbol{\Sigma}\boldsymbol{H}^{\boldsymbol{H}}(f) \qquad [7]$$

where $\boldsymbol{H}^{\boldsymbol{H}}(f)$ is the Hermitian of $\boldsymbol{H}(f)$ and $\boldsymbol{\Sigma} = diag([\sigma_1^2 \quad \dots \quad \sigma_M^2])$ is the covariance matrix of the process noise $\boldsymbol{\varepsilon}$. Based on the power spectral density matrix, we can generate smoothed versions of the power spectral density of the signals under consideration using the MVAR model as interpolating function.
The transfer matrix, the coefficient matrix as well as the power spectral density matrix can be also used to extract various coupling and causality measures such as coherence (COH) [11], directed coherence (DC) [12], partial coherence (PCOH) [13] and partial directed coherence (PDC) [14]. For the purposes of this work, we only considered DC, which describes causality as direct and indirect power contributions from one time-series to the other. DC from time-series D (i.e., driver) to time-series T (i.e., target) ($D \rightarrow T$) at frequency f is computed as [12],

$$DC_{TD}(f) = \frac{\sigma_D \cdot H_{TD}(f)}{\sqrt{\sum_{m=1}^{M} \sigma_m^2 \cdot |H_{Tm}(f)|^2}} \qquad [8]$$

The total information outflow from a particular region can be defined as the sum of statistically significant connections (e.g., DC values) towards all other cortical regions [1],

$$Outflow_D(f) = \sum_{T=1,T\neq D}^{M} DC_{TD}{}^{*}(f) \qquad [9]$$

where $DC_{TD}{}^{*}(f)$ refers to statistically significant DC values from time-series D to time-series T. To evaluate statistical significance, we permuted randomly 50 times the order of the source signals in each trial and estimated MVAR models based on the acquired trials. This way we destroyed possible

Published by Verlag der TU Graz
Graz University of Technology

DOI: 10.3217/978-3-85125-826-4-20

causal interactions between different regions and generated a reference DC distribution under the null hypothesis of no ''causality'' from time series D to T. The significance of the DC values evaluated from the actual data was then assessed using the reference DC distribution. The estimated DC and outflow values were finally averaged over different cortex areas. The 12 regions of interest (ROI) were the left and right hemisphere somatosensory, broca's, primary motor, pre-motor, visual and perirhinal areas.

Results

The MVAR framework was applied on two different time periods: before and after cue onset. The optimal model order (*p*) varied from 7-9 (for a sampling rate of 256Hz and for different MVAR models fitted on different attempted movements). The estimated DC values averaged over different type of attempted movements in the frequency range of [0.3 70] Hz can be found in Fig. 2. In the depicted matrices the columns and rows represent the driver and target ROIs, respectively. For example, the first column is the DC from left hemisphere (L) somatosensory area to all other regions (denoted in the y-axis of the matrix). Figure 3 illustrates the total information outflow (Eq. 9) from each ROI in different frequency bands (*delta* [0.3-4] Hz, *theta* [4-7] Hz, *alpha* [8-14] Hz, *beta* [14-32] Hz, *gamma* [32-60] and *broad* [0.3-70] Hz) and for different type of attempted movements before and after cue onset.

The obtained results were subjected to a three-way analysis of variance (ANOVA) examining the effect of attempted movement, frequency band and ROI on the DC changes before and after cue onset (i.e., the dependent variable was defined as $DC_{TD}(f)^{(after\ cue\ onset)} - DC_{TD}(f)^{(before\ cue\ onset)}$). The resulting *p*-values for the independent variables and their interactions can be found in Tab. 1.

Table 1: Three-way ANOVA examining the effect of attempted movement, frequency band and ROI on the DC changes after cue onset. $p < 0.05$ indicates strong effects.

Source	*p*-value
Attempted movement	0.086
Frequency band	0.011
ROI	0
Attempted movement $*$ Frequency band	0.984
Attempted movement $*$ ROI	0
Frequency band $*$ ROI	0

Discussion

Figs. 2 and 3 provide important information regarding the main sources/hubs of information. We detected overall increased outflow from the somatosensory and primary motor areas before and after cue onset. The outflow from the somatosensory area was elevated mainly in the beta and alpha band, whereas the outflow from the primary motor cortex was more pronounced in the delta band. The somatosensory area outflow was overall higher prior to cue onset. In contrast, the primary motor area outflow increased after cue onset, especially in the delta band. The main receivers of somatosensory information were the primary motor, the broca's, the perirhinal and the somatosensory area itself. On the other hand, the main receivers of primary motor information were the visual, the perirhinal and the somatosensory area. We also detected an ipsilateral pattern whereby dominant sources of information originated mainly from the right hemisphere.

Based on Fig.3, the outflow from different ROIs and for different type of attempted movements exhibited similar characteristics. However, we detected significant differences in DC changes before and after cue onset (Tab. 1). The three-way ANOVA returned a *p*-value of 0.086 (i.e., weak effect) for the factor 'attempted movement' and a *p*-value of 0 (i.e., strong effect) for the interactions between 'attempted movement' and 'ROI', indicating that the mean DC change can be explained better when considering both type of movement and driving ROI. An important aspect that should be pointed out here is that the exact attempt onset after the cue is not exactly known and this could also affect the results (i.e., the effect of the factor 'attempted movement' by itself could be more significant).

Conclusions

We estimated directional connectivity and information flow in SCI subjects during attempted hand and arm movements. Our results indicate that the most prominent sources of information were the somatosensory area prior to cue onset (in the beta/alpha band) and the primary motor area after cue onset (mainly in the delta band). DC and outflow measures exhibited the same patterns for different type of attempted movements. However, DC changes before and after cue onset in different ROIs were more informative in terms of the type of movement attempted by the SCI participant. This implies that the time- and spatial- varying aspects of DC could be used as features to improve decoding performance in BCI applications [5]. Future work involves DC estimation in a time-varying (TV) context using nonstationary MVAR models [2] and attempted movement classification using various TV-MVAR based connectivity measures.

References

[1] L. Astolfi *et al.*, "Comparison of different cortical connectivity estimators for high-resolution EEG recordings," *Hum. Brain Mapp.*, vol. 28, no. 2, pp. 143–157, 2007.

[2] K. Kostoglou *et al.*, "A novel framework for estimating time-varying multivariate autoregressive models and application to cardiovascular responses to acute exercise," *IEEE Trans. Biomed. Eng.*, pp. 1–1, 2019, doi: 10.1109/TBME.2019.2903012.

DOI: 10.3217/978-3-85125-826-4-20

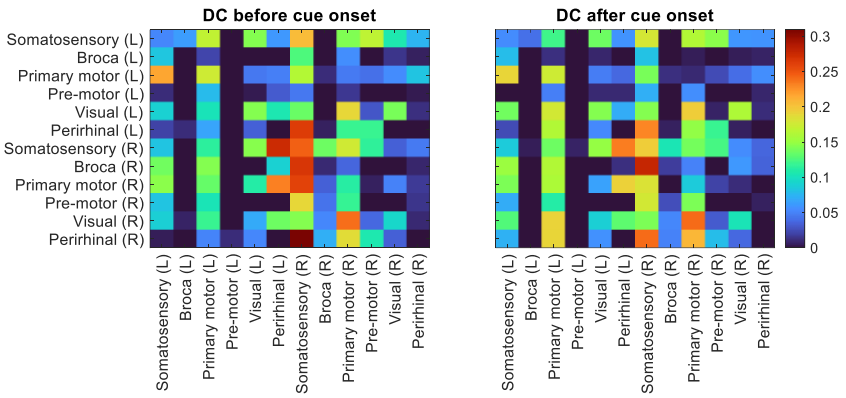

Figure 2: Averaged DC values over all attempted movements before (left panel) and after (right panel) cue onset in the frequency range of [0.3 70Hz]. The columns represent the drivers and the rows the targets. (L) and (R) refers to left and right hemisphere.

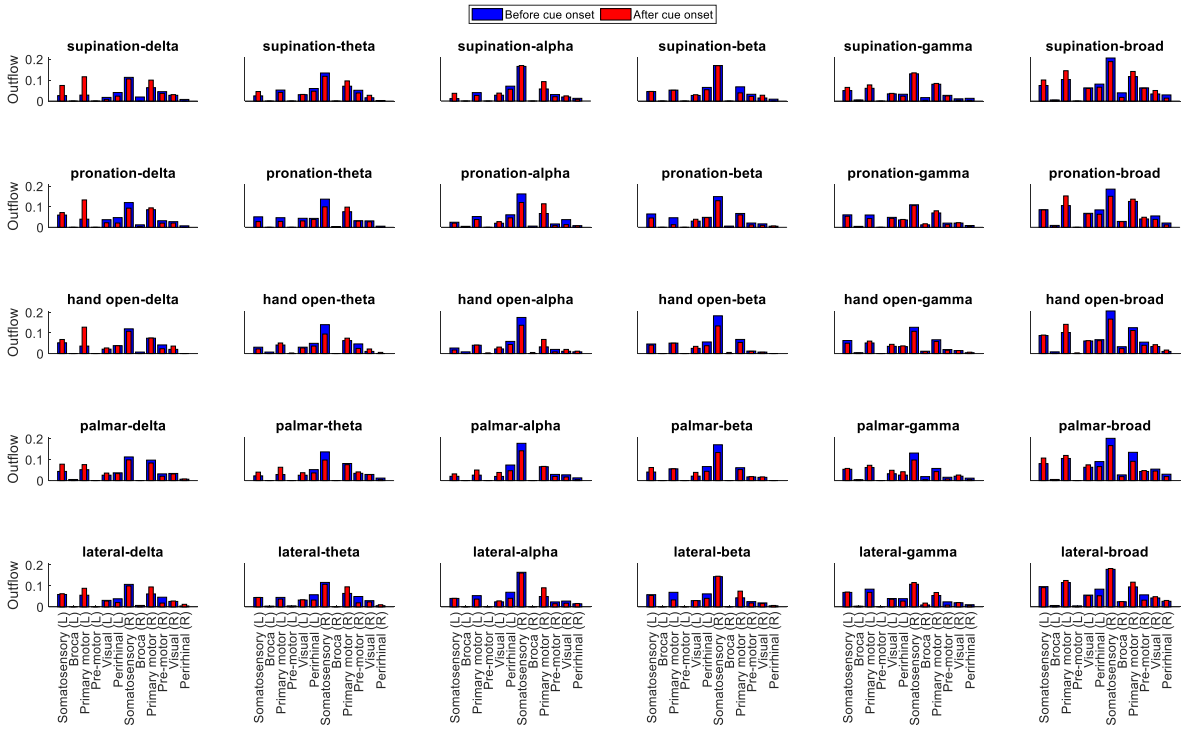

Figure 3: Total information outflow before (blue) and after (red) cue onset in the delta (first column), theta (second column), alpha (third column), beta (fourth column), gamma (fifth column) and broad (sixth column) and for different type of attempted movements i.e., supination (first row), pronation (second row), hand open (third row), palmar grasp (fourth row) and, lateral grasp (fifth row).

[3] L. Faes and G. Nollo, “Multivariate frequency domain analysis of causal interactions in physiological time series,” in *Biomedical Engineering, Trends in Electronics, Communications and Software*, InTech, 2011.

[4] S. Shoham *et al.*, “Motor-cortical activity in tetraplegics,” *Nature*, vol. 413, no. 6858, p. 793, 2001.

[5] P. Ofner *et al.*, “Attempted Arm and Hand Movements can be Decoded from Low-Frequency EEG from Persons with Spinal Cord Injury,” *Sci. Rep.*, vol. 9, no. 1, pp. 1–15, 2019.

[6] G. R. Müller-Putz *et al.*, “Towards non-invasive brain-computer interface for hand/arm control in users with spinal cord injury,” *2018 6th Int. Conf. Brain-Computer Interface, BCI 2018*, vol. 2018-Janua, pp. 1–4, 2018.

[7] L. Astolfi *et al.*, “Study of the time-varying cortical connectivity changes during the attempt of foot movements by spinal cord injured and healthy subjects,” *Proc. 31st Annu. Int. Conf. IEEE Eng. Med. Biol. Soc. Eng. Futur. Biomed. EMBC 2009*, pp. 2208–2211, 2009, doi: 10.1109/IEMBS.2009.5334878.

[8] F. Tadel *et al.*,, “Brainstorm: a user-friendly application for MEG/EEG analysis,” *Comput. Intell. Neurosci.*, vol. 2011, 2011.

[9] H. Lütkepohl, *New introduction to multiple time series analysis*. Springer Science & Business Media, 2005.

[10] L. Faes, S. Erla, and G. Nollo, “Measuring connectivity in linear multivariate processes: definitions, interpretation, and practical analysis,” *Comput. Math. Methods Med.*, vol. 2012, 2012.

[1 1] S. M. Kay, *Modern spectral estimation*. Pearson Education India, 1988.

[12] L. A. Baccala *et al.*, “Studying the interaction between brain structures via directed coherence and Granger causality,” *Appl. Signal Process.*, vol. 5, no. 1, p. 40, 1998.

[13] K. Yacoub, “Relationship between multiple and partial coherence functions,” *IEEE Trans. Inf. Theory*, vol. 16, no. 6, pp. 668–672, 1970.

[14] L. A. Baccalá, K. Sameshima, and D. Y. Takahashi, “Generalized partial directed coherence,” in *2007 15th International Conference on Digital Signal Processing*, 2007, pp. 163 –166.

Published by Verlag der TU Graz
Graz University of Technology